Mechanical and Thermal Properties of Epoxy Polymethyl Methacrylate Blends Synthesized in Supercritical Carbon Dioxide

M. G. H. Zaidi,[1] N. Bhullar,[1] V. P. Singh,[2] P. L. Sah,[2] S. Alam,[3] R. Singh[4]

[1]*Supercritical Fluid Processing Laboratory, Department of Chemistry*
[2]*Department of Mechanical Engineering, G. B. Pant University of Agriculture & Technology, Pantnagar Uharanehal 263145, India*
[3]*Polymer Division, Defense Material Stores Research Development & Establishment, Kanpur 208013, India*
[4]*Directorate of Extramural Research and Intellectual Property Rights, New Delhi 110011, India*

Received 31 May 2006; accepted 31 July 2006
DOI 10.1002/app.25272
Published online in Wiley InterScience (www.interscience.wiley.com).

ABSTRACT: A series of epoxy/polymethyl methacrylate (E/PMMA) blends was synthesized through impregnation polymerization of methyl methacrylate at concentrations ranging (0–1.5 phr) into diglycidyl ether of bisphenol-A (0.1 mol) in presence of 2,2-azobisisobutyronitrile (2×10^{-2} mol) at 3000 psi, (60–90 ± 1)°C for 3 h in supercritical carbon dioxide, followed by curing of treated epoxy with triethylene tetramine (10 phr) at (40 ± 1)°C. The progress of all such impregnation polymerization reactions was monitored rheoviscometrically. Formation of E/PMMA blends was ascertained through of PMMA mass uptake (%) into epoxy, UV–vis and FTIR spectra, and TEM. With PMMA mass uptake (%), compression strength and resistance against wear of E/PMMA blends were increased with simultaneous decrease in their Rockwell hardness (R scale), charpy impact, and tensile strength, respectively. All E/PMMA blends have shown non-uniform photoelastic behavior at applied load ranging 4–20 kgf and significant stability against thermooxidation with T_g/T_m and char yield (%) ranging 0.53–0.59, 29.31–31.66, respectively.
 J Appl Polym Sci 103: 1303–1310, 2007

Key words: supercritical carbon dioxide; polymer blends; impregnation polymerization; spectra; TEM; mechanical properties; TG-DTA-DTG

INTRODUCTION

Over the past few decades, supercritical fluids including supercritical carbon dioxide ($scCO_2$) has gained significant technological incentives due to their gas-like diffusivity and liquid-like density. Unique property of diffusion of $scCO_2$ increases the free volume and mobility of the polymer chains with simultaneous reductions in the glass transition temperature and viscosity. This has opened opportunity to synthesize and process a variety of materials ranging from nanoparticles to polymer-based composites, particularly polymer blends in $scCO_2$.[1–3] In this connection, a variety of polymer blends with improved mechanical and thermal properties has recently been synthesized through either of mixing of two or more immiscible polymers with each other in a nonreactive or reactive manner in $scCO_2$. Since, the reduction in viscosity is different for different polymers depending on the amount of $scCO_2$ applied under given processing conditions, the viscosity ratio of the polymer formulations has also been manipulated during the formation of their blends in $scCO_2$.[2–6]

A reactive route based on impregnation or *in situ* polymerization for producing polymer blends involves $scCO_2$ assisted infusion of reagents (monomer and initiator) into host polymer or followed by subsequent polymerization reaction. In this route, $scCO_2$ impart swelling that enhances the diffusion of reagents and hence, high molecular weight polymer can be synthesized in the host polymer. The main advantage of this route is that the mass uptake of a polymer formed by reaction in the host can be controlled through variables such as pressure, soaking time and monomer concentration control, and the total mass uptake of reagents. In this process, polymerization also takes place at the surface of the host polymer. However, the amount of polymer synthesized within the host polymer is always much larger. Several polymer blends with high mass uptake and better distribution of the minor component in the major component have been prepared using the reactive route. In this connection, although polymerization of a variety of vinyl functional monomers within a range of host polymers, including poly(chlorotriuoroethylene), poly(4-methyl-1-pentene) polyethylene, bisphenol A polycarbonate, poly(oxymethylene),

Correspondence to: M. G. H. Zaidi (mgh_zaidi@yahoo.com).
Contract grant sponsor: Government of India; contract grant number: ERIP/ER/0403449/M/01.

and nylon-6,6 has been reported,[2,3–8] and no significant efforts has been made to synthesize epoxy/thermoplastic blends in $scCO_2$. Conventional synthesis of such epoxy thermoplastic blends through solution phase or melt-blending procedures is carried out either in presence of toxic and flammable solvents or melt processing at high temperatures to improve the mechanical and thermal properties of the highly crosslinked epoxies. The composition and curing conditions determine the morphology of the cured system, which settles the final mechanical and thermal properties of epoxy/thermoplastic blends.[9]

Following the experimental results reported on thermal polymerization of methyl methacrylate (PMMA)[10] and separation of PMMA phase from polystyrene matrix in $scCO_2$,[11] in the present investigation, efforts have been made to synthesize epoxy/polymethyl methacrylate (E/PMMA) blends through impregnation polymerization of methyl methacrylate (MMA) into diglycidyl ether of bisphenol A (DGEBA) initiated with 2,2-azobisisobutyronitrile (AIBN) in $scCO_2$,[6–8,12] followed by curing of the resulting DGEBA/PMMA composition with triethylene tetramine (TET) as phase separating agent.[9] The progress of impregnation polymerization has been monitored rheoviscometrically.[13] The formation of E/PMMA blends has been ascertained through mass uptake (%) of PMMA into epoxy, UV–vis, and FTIR spectra. Effect of PMMA mass uptake (%) on the surface morphology of E/PMMA blends was ascertained through transmission electron microscopy. Mechanical properties of all such E/PMMA blends were studied through variations in their wear behavior at four different combinations of hydraulic end loadings, disc speeds, compression strength, impact strength, tensile strength, Rockwell hardness (R scale), and photoelastic behavior under applied load ranging 4–20 kgf. Stability of E/PMMA blends against thermooxidation and, various thermal parameters was studied through simultaneous thermogravimetric-differential thermal analysis-differential thermogravimetry (TG-DTA-DTG).[3–6,14]

EXPERIMENTAL

Materials

The commercially available methyl methacrylate (MMA) from Ms CDH chemicals, India, was purified through distillation under reduced pressure (λ_{max}, 259 nm). Diglycidyl ether of bisphenol A (DGEBA) and triethylene tetramine (TET) were purchased from Ms Cibatul, India. Epoxy equivalent of DGEBA (197 g/equiv) was deduced according to pyridinium chloride method.[14]

Measurements

UV–vis spectra were recorded on Genesis 10 thermospectronic spectrophotometer in chloroform. FTIR spectra were recorded on Bucker FTIR Spectrophotometer in KBr. Transmission electron micrographs (TEM) of specimens were recorded over Philips EM-400 at 45 mA and 1.82 Kev at a camera length 290 mm, having exposure time 1.7 s. Wear behavior of blends was studied at different combinations of hydraulic end loading and disc speeds using pin on disc machine TE-97/7050 (750 W, 3 phase) with 14 spindle speeds ranging 25–2150 rpm and fitted with Muyford super lathe, dead weight tester, and transducer with calibration 0.892 m v/v. Compression strength of blends (kgf/cm^2) was recorded over Tinus Olson universal testing machine (UTM). Impact strength (kgf m) of E/PMMA blends was directly recorded over UTM as energy required inducing a visible crack. Tensile strength of specimens was directly recorded on the dial gauge over Instron UTM at the test specimen gauge length 55 mm, diameter 20 mm, total shoulder length 200 mm, and end diameter 25 mm. The specimen elongations were also directly recorded on linear scale. Hardness of the specimen was recorded in terms of R scale over Rockwell hardness testing machine with ball indenter (1/2″, 12.70 mm) at the minor load of 10 kg. Photoelastic analysis of the specimens was carried out over a circular disc of 75 mm diameter and 5 mm thickness loaded under diametric compression on the standard circular polariscope. The fringe order at the center of the disc was determined.[15] The rheoviscometric measurements were carried out on a Nach Hoppler Viscometer Viscosity, and is derived from the resistance against the resin. When the ball sinks 30 mm deep in the cuvette, the time was measured.[13] Simultaneous differential thermogravimetry-thermogravimetry-differential thermal analysis (DTG-TG-DTA) was performed over Netzsch-Geratebau GmbH thermal analyzer model STA-409 in static air at 25°C/10 (K/min)/1000°C. Density of E/PMMA blends was deduced according to ASTM D 792-66 1970 and the density data was used for calculations of PMMA mass uptake (%) into epoxy.[16]

Synthesis of E/PMMA blends in $scCO_2$

All E/PMMA blends were synthesized in a stainless steel high pressure reactor (100 cm^3), manufactured by Pressure Products Industries, USA, equipped with PID temperature controller.[7,11,12] The reactions were stirred by a mechanical stirrer bar at 1000 rpm. Carbon dioxide (99.99%) was delivered directly to the reaction cell at the desired pressure. The system pressure was measured by a pressure gauge. The temperature inside the cell was measured by an industrial insulated thermocouple provided and displayed on PID temperature controller. The reactor was heated with an electrical heating tape wrapped around the exterior of the cell. Degassed DGEBA (0.1 mol) and

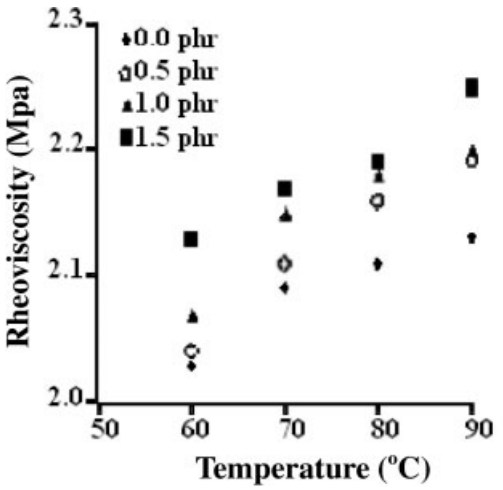

Figure 1 Effect of impregnation polymerization of methyl methacrylate (MMA) at 3000 psi in $scCO_2$ on rheoviscosity of PMMA/DGEBA formulations in chloroform at 0.5 g/dL, at (25 ± 1)°C.

AIBN (2×10^{-2} mol) were added under N_2 to the stainless steel cell containing the specified amount of MMA (0–1.5 phr), and which had been previously purged with N_2. The cell was initially pressurized with carbon dioxide, and then gradually heated within temperature range (60–90 ± 1)°C to obtain the desired pressure of 3000 psi. The reaction mixture was stirred in $scCO_2$ for 3 h. The cell was cooled to (40 ± 1)°C and the CO_2 was vented into dichloromethane. The cell was opened to give DGEBA/PMMA formulations as thick pale yellow liquids. Progress of impregnation polymerization of MMA into DGEBA was monitored in chloroform rheoviscometrically with reference to DGEBA at the concentration of 0.5 g/dL at (25 ± 1)°C (Fig. 1). The E/PMMA formulations synthesized at (90 ± 1)°C were subsequently cured with TET (10 phr) and fabricated into different dimensions for their mechanical characterizations (Table I). PMMA as reference was also synthesized under similar conditions in $scCO_2$.[10]

RESULTS AND DISCUSSION

Synthesis of E/PMMA blends in $scCO_2$

A series of E/PMMA blend was synthesized through 2,2-AIBN (2×10^{-2} mol) initiated impregnation polymerization of MMA at various concentrations ranging (0–1.5 phr) into diglycidyl ether of bisphenol-A (0.1 mol) at temperature ranging 60–90°C in $scCO_2$, followed by curing of the resulting DGEBA/PMMA formulations with TET (10 phr). This has afforded E/PMMA blends with increasing density in the range of 1.1603–1.1798, corresponding to PMMA mass uptake (%) 0.7670–1.6806. All such impregnation polymerization reactions were monitored rheoviscometrically to achieve the corresponding E/PMMA blends with enhanced PMMA mass uptake (%). With the increase in temperature, the rheoviscosity of DGEBA/PMMA formulations measured at concentration of 0.5 g/dL in chloroform at (25 ± 1)°C was increased ranging 2.03–2.25 (Mpa s) with maximum for the set of impregnation polymerization executed at (90 ± 1)°C (Fig. 1). DGEBA/PMMA formulations synthesized at (90 ± 1)°C were cured with TET (10 phr), and the resulting E/PMMA blends were investigated for their spectra, morphology, thermal, and mechanical properties.

Spectra

To get an insight into the affinity of PMMA, with the composite, [I_0] formed as a result of curing of DGEBA with TET, synthesized E/PMMA blends were studied for their UV–vis and FTIR spectra. PMMA synthesized at 3000 psi in $scCO_2$ showed absorption at 230 nm. DGEBA showed absorption at 257 nm that was blue shifted to 230 nm due to $\pi - \pi^*$ transition, corresponding to the formation of a pair of auxochromes as —OH and —NH— for [I_0]. With increase in PMMA mass uptake (%), wavelength maxima corresponding to E/PMMA blends were increased, ranging 230–239 nm with maximum at 239 nm, corre-

TABLE I
Effect of PMMA Mass Uptake (%) into Epoxy in $scCO_2$ on Mechanical and Thermal Properties of Properties of E/PMMA Blends

	[Io]	[I]	[II]	[III]
MMA concentration (phr)	0.00	0.50	1.00	1.50
PMMA mass uptake (%)	0.0	0.7670	0.9652	1.6806
Density (ASTM D 792-66 1970)	1.1603	1.1992	1.1715	1.1798
Compressive strength (kgf/cm^2)	159.40	168.01	176.85	178.62
Charpy impact strength (10^{-2} kgf m)	6.30	7.50	5.50	5.00
Tensile strength (kgf/cm^2)	255.60	130.88	172.79	173.44
Rockwell hardness (RH scale)	115.00	110.00	108.00	107.00
Fringe value (10^{-2} kgf/fringe cm)	944.50	603.70	958.00	895.00
T_g/T_m	0.53	0.55	0.54	0.59
Char yield (%)	29.31	29.43	31.12	36.66

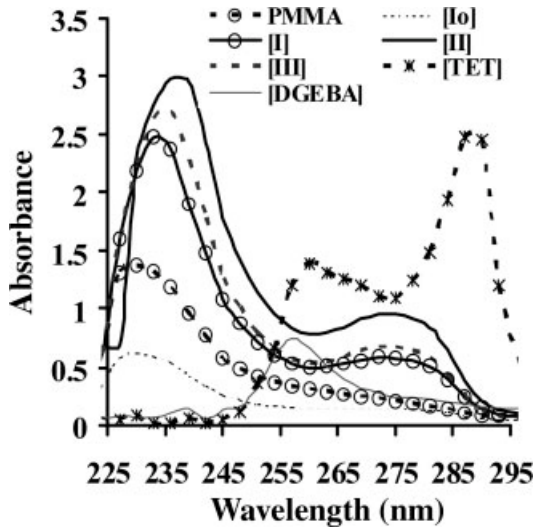

Figure 2 UV–vis spectra of E/PMMA blends.

sponding to [II] due to $\pi - \pi^*$ transition. This has also contributed to the increase in absorbance ranging 0.605–2.952 with maximum absorbance, corresponding to [II] in UV region (Fig. 2). FTIR spectra has also reflected the formation of —OH group due to condensation of amino group of TET with epoxy group of DGEBA in all the E/PMMA blends along with amide linkages due to the condensation of amino group of TET with ester linkage of PMMA. The reference [I_0] synthesized in the absence of MMA shows a wide band at 3426.66 cm^{-1} corresponding to ν_{O-H} that was shifted to lower frequency at 3409.55 and 3400.05, corresponding to the [I] and [II], due to the existence of intermolecular hydrogen bonded —OH groups. A shift of ν_{O-H} from the standard data (3550–3200 cm^{-1}) to 3426.66 $\times$ 123.34 cm^{-1} corresponds to medium level intramolecular hydrogen bonding formed between the adjacent —OH and —NH groups in [I_0]. A well-defined band corresponding to ν_{N-H} was appeared at 3045.72 for [I], whereas in rest of E/PMMA blends, it was merged with their respective ν_{O-H}. Band at 2960.58 cm^{-1}, corresponding to ν_{C-H} for $-CH_3$ group of bisphenol-A component of DGEBA, was merged with ν_{C-H} of aromatic ring. New band corresponding to $\nu_{C=O}$ was appeared for [I] at 1727.95 cm^{-1}, and [III] at 1724.35 cm^{-1} indicated the distribution of PMMA component into E/PMMA blend. PMMA component was derivatized into the corresponding amide during the curing process in presence of TET, due to which a band for [I] at 1607.62 $cm^{-1}$and [III] at 1609.14 cm^{-1} was appeared corresponding to ν_{CONH}.[17] These spectral observations clearly indicate that amino groups of TET were simultaneously condensed with epoxy group of DGEBA and ester groups of PMMA thus impart a TET crosslinked structure to the synthesized E/PMMA blends (Fig. 3).

Morphology

Typical transmission electron micrographs at magnification level 2500, which are shown, reveal the phase morphology development of thin films casts of E/PMMA blends synthesized at 0.5 and 1.5 phr in $scCO_2$ (Fig. 4). Bright phase in transmission electron micrographs indicate the dispersed phase corresponding to TET cured DGEBA and the dark phase corresponds to the rich phase due to phase separation caused by addition of TET and or PMMA. The E/PMMA blend synthesized at MMA concentration 0.5 phr has shown phase separation, as indicated by the dark phase [Fig. 4(a)]. With the increase in the MMA concentration to 1.5 phr, the epoxy rich phase becomes brighter and the PMMA rich phase develops into the darker [Fig. 4(b)]. These observations indicate that the synthesized E/PMMA blends have morphology with separated PMMA phase in the synthesized blends.[18]

Mechanical properties

With increase in MMA concentration, the corresponding E/PMMA blends have shown an increase in the compression strength (kgf/cm^2) ranging 159.40–178.62 with simultaneous decrease in Rockwell hardness ranging 115.0–107.0 of E/PMMA blends. The composite [I_0] has shown compression strength 159.40. This was increased to 168.01 corresponding to E/PMMA blend synthesized at MMA concentration 0.50 phr. With further increase in MMA concentration to 1.0 phr, the corresponding E/PMMA blend has shown a remarkable increase in compressive strength to 176.85 that was slightly increased to 178.62 at MMA concentration 1.5 phr. Although TEM reveled the morphology of E/PMMA blends with separated PMMA phase (Fig. 4), such increase in compressive strength

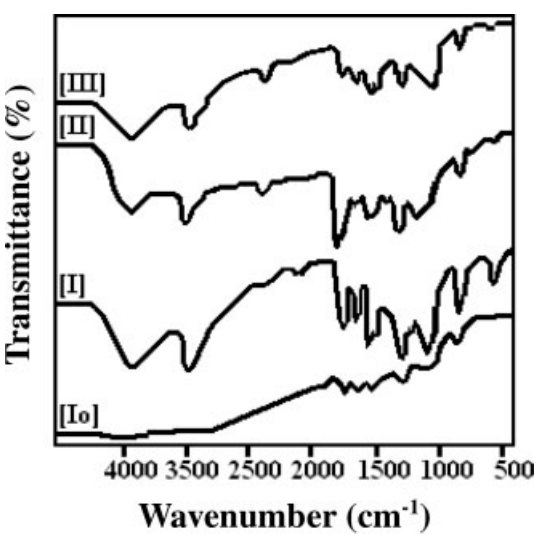

Figure 3 FTIR spectra of E/PMMA blends.

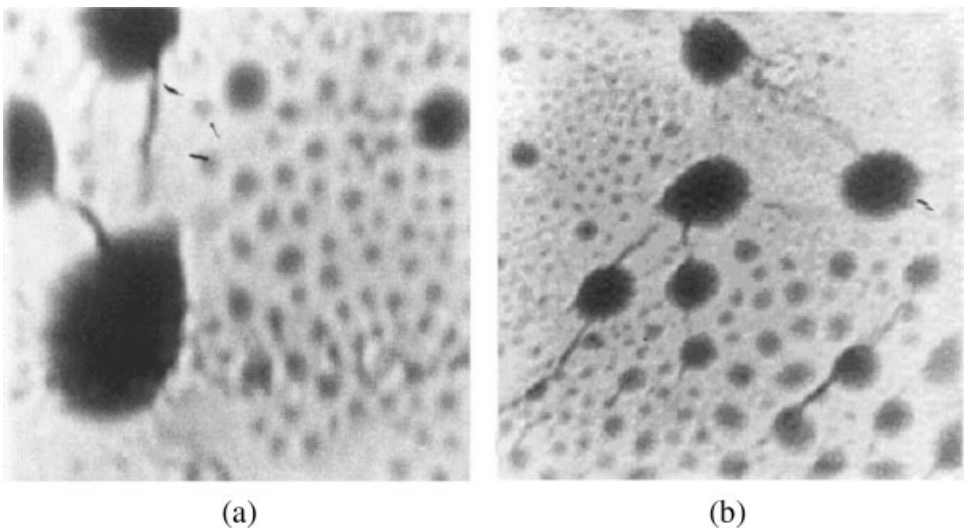

Figure 4 (a) Transmission electron micrograph of [I] at ×2500. (b) Transmission electron micrograph of [III] at ×2500.

in E/PMMA blends with MMA concentration may be due to the formation of a crosslinked structure through amide linkage formation due to the condensation of ester group of PMMA with amino group of TET as observed in FTIR spectra (Figs. 2 and 3). The composite [I_0] has shown Charpy impact strength (kgf m × 10^{-2}) 6.30. This was increased to 7.50 corresponding to E/PMMA blend [I]. With further increase in PMMA mass uptake, a rapid loss in the charpy impact strength was observed with lowest at 5.50 for [III]. In contrast to charpy impact strength, the tensile strength of E/PMMA blends was first decreased to 130.88 corresponding to [I], thereafter increased to a stagnating value of 173.44 corresponding to [III] (Table I).

Effect of PMMA mass uptake on the wear behavior or of E/PMMA blends was studied at four different combinations of hydraulic end loadings (bar)/and disc speeds (rpm). The respective wear volume (W_v, mm^3) of E/PMMA blends were recorded corresponding to 60 s. At each of the combinations, the W_v (mm^3) of E/PMMA blends was increased with hydraulic end loadings/disc speeds. The composite [I_0] has shown W_v 2.75 mm^3 at 1.0 bar/232 rpm. Increase in disc speed to 322 rpm has imparted increase in W_v to 3.47, which was stagnated to 1.5 bar at 232 rpm. With increase in disc speed to 322 rpm, [I_0] has shown a sharp increase in W_v to 4.20 mm^3. The E/PMMA blend [I] synthesized at MMA concentration 0.5 phr has shown W_v appreciably lower than [I_0] at all the

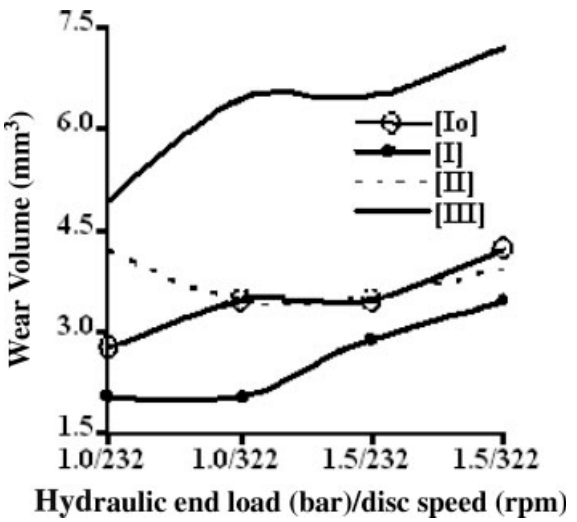

Figure 5 Wear behavior of E/PMMA blends in 60 s at different combinations of hydraulic end loadings and disc speeds.

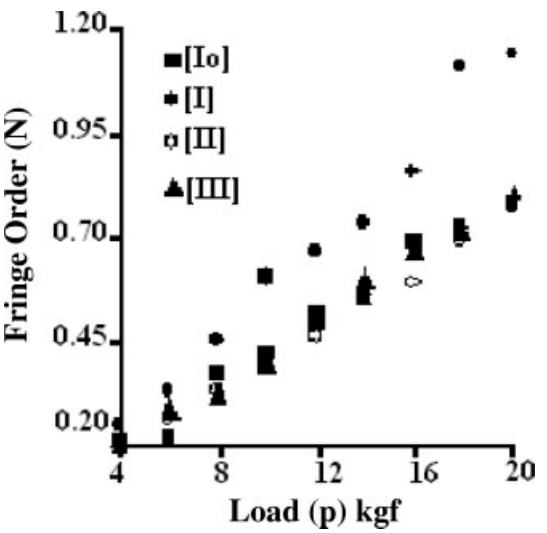

Figure 6 Effect of PMMA uptake on fringe order of E/PMMA blends.

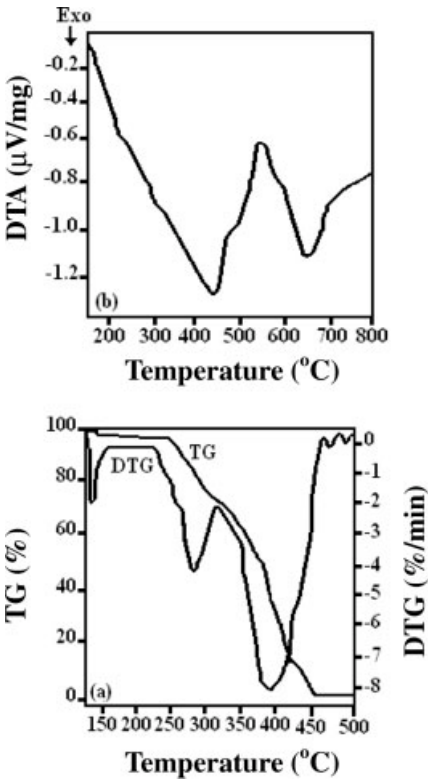

Figure 7 TG-DTG (a) and DTA (b) scans of PMMA synthesized at 3000 psi in $scCO_2$.

combinations of hydraulic end loadings/disc speeds. At 1.0 bar/232 rpm, [I] has shown W_v 2.03 mm^3, which was stagnated up to 322 rpm. With increase in hydraulic end load of 1.5 bar, W_v for [I] was increased to 2.89 mm^3, that was further increased to 3.48 mm^3 with increase in disc speed of 322 rpm. The values of W_v for E/PMMA blends [II] and [III] were higher than [I_0] as well as [I]. These observations clearly indicate that E/PMMA blend synthesized at MMA concentration 0.5 phr has contributed appreciable control in wear behavior due to decrease in W_v up to 1.0 bar/322 rpm [Fig. 5]. The fringe order of E/PMMA blends was studied at various applied load ranging 4–20 kgf (Table I). All such E/PMMA blends have shown irregular trend in fringe order ranging 944.5–958.0 with maximum value for [II]. Such an irregular fringe order may be due to the nonuniform distribution of PMMA into E/PMMA blends, which is also indicated in their transmission electron micrographs (Figs. 4 and 6).

Thermal stability

With PMMA mass uptake, all E/PMMA blends have shown increasing thermooxidative stability and characteristic profiles for glass transition temperature (T_g), melting temperature (T_m), and oxidation temperature (T_{ox}). PMMA was decomposed in two steps with first

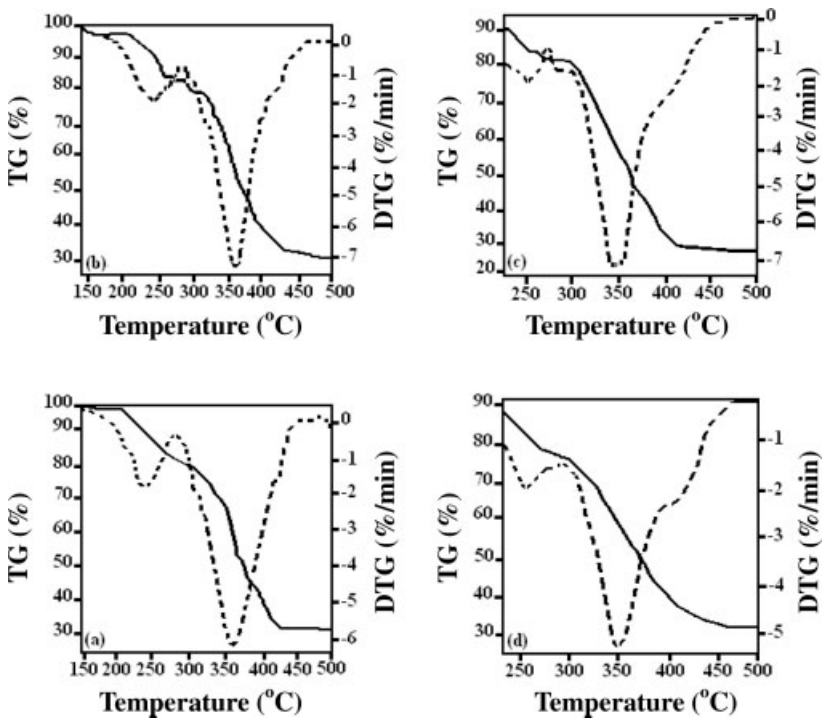

Figure 8 TG-DTG scans of TET cured DGEBA (a), and E/PMMA blends synthesized at MMA concentration 0.5 phr (b), 1.0 phr (c), and 1.5 phr (d) at 3000 psi in $scCO_2$ (a): *X* axis: temperature (°C) and left *Y* axis: TG (%) and right *Y* axis: DTG (%/min) (b): *X* axis: temperature (°C) and left *Y* axis: TG (%) and right *Y* axis: DTG (%/min) (c): *X* axis: temperature (°C) and left *Y* axis: TG (%) and right *Y* axis: DTG (%/min) (d) *X* axis: temperature (°C) and left *Y* axis: TG (%) and right *Y* axis: DTG (%/min).

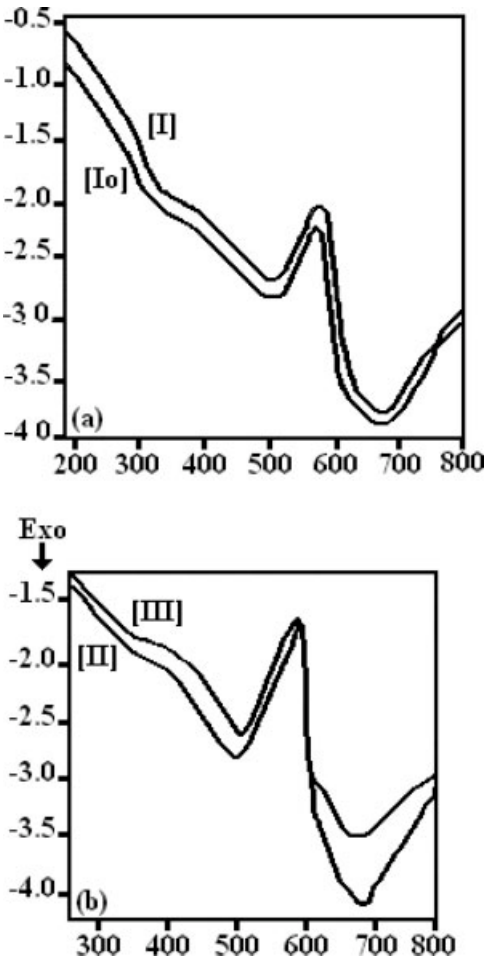

Figure 9 Effect of PMMA mass uptake (%) on DTA spectra of E/PMMA blends; *X* axis: temperature (°C) and *Y* axis: DTA (μV/mg).

step started at 281.9°C corresponding to 16.5% weight loss. This was smoothly progressed up to the second step decomposition appeared at 394.7°C with 32.0% weight loss [Fig. 7(a)]. DTA spectrum of PMMA indicates profile corresponding to T_g: 431.4°C, T_m: 552.2°C, and T_{ox}: 653.0°C [Fig. 7(b)]. The composite [I_0] also decomposes in two steps. First decomposition of [I_0] was observed at 238.3°C with 8% weight loss. The second-step decomposition of [I_0] was observed at 355.4°C with 40% weight loss [Fig. 8(a)]. The EPMMA blend [I] and [II] were also decomposed in two steps with almost same as TG-DTG profiles [Figs. 8(b–c)]. First-step decomposition of [I] was observed at 243.2°C with relatively higher weight loss of 12% than [I_0]. The second step decomposition of [I] was observed at 350.8°C with 39.8% weight loss almost similar to [I_0]. In contrast to [I]and [II], the E/PMMA blend [III] was decomposed in three steps. At first step, [III] was decomposed at 247.4°C, the temperature higher than the remaining composites. At this stage, the corresponding weight loss associated with [III] was 15.7%. Decomposition of [III] was observed at 350.8°C corresponding to second step with weight loss 32.5%, that was subsequently extended to 62% at 407.8°C corresponding to the third-step decomposition temperature [Fig. 8(d)]. Such increase in thermooxidative stability of E/PMMA blends may be attributed to the formation of amide linkage, which bears a very high value of cohesive energy than carboxy linkage of the ester group.[13] For many polymers, the value of T_g/T_m ranges from 0.53 to 0.59.[19] Crystalline polymers may therefore display both T_g corresponding to long-range segmental motion in the amorphous region and a crystalline melting temperature T_m, at which crystallites are destroyed and an amorphous, disordered melt is formed. PMMA has shown T_g/T_m as 0.53, which was slightly lower to [I_0] where it was 0.55. With PMMA mass uptake, T_g/T_m corresponding to [I] and [II] were 0.55. With further increase in PMMA concentration, this ratio was increased to 0.59 indicating the increase in the amorphous character of E/PMMA blends with PMMA concentration.[19] With PMMA mass uptake, the char yield (%) of E/PMMA blends was increased ranging 29.31–36.66. Such increase in char yield clearly reflects about the effect of PMMA mass uptake on flame retardant characteristics of the synthesized E/PMMA blends.[19] The composite [I_0] has shown char yield (%) 29.31, which was slightly enhanced to 29.42 corresponding to E/PMMA blend [I] synthesized at MMA concentration 0.5 phr. With increase in MMA concentration to 1.0 phr, the corresponding increase in char yield in E/PMMA blend [II] was 31.52, that was further increased to 36.66 for E/PMMA blend [III] synthesized at MMA concentration 1.5 phr. These observations clearly indicate that PMMA mass uptake has significantly enhance the thermooxidative stability and thermal properties of E/PMMA blends.

CONCLUSIONS

Synthesis of E/PMMA blend was successfully accomplished through impregnation polymerization of MMA at different concentrations ranging (0–1.5 phr) into diglycidyl ether of bisphenol-A (0.1 mol) initiated with 2,2-azobisisobutyronitrile (2×10^{-2} mol) at 3000 psi, (60–90 ± 1)°C for 3 h in supercritical carbon dioxide, followed by curing of treated epoxy with triethylene tetramine (10 phr) at (40 ± 1)°C. Monitoring of all such impregnation polymerization reactions at 0.5 g/dL in chloroform at (25 ± 1)°C reveled their rheoviscosity ranging 2.03–2.25 Mpa s. This has afforded corresponding E/PMMA blends with PMMA mass uptake (%) into epoxy ranging 0.7670–1.6806. UV–vis and FTIR spectra has reveled the formation of E/PMMA blends. Separation of PMMA phase into epoxy has clearly been observed in epoxy in transmission electron micrographs. All E/PMMA blends have shown nonuniform variations in

material fringe value with lowest wear volume for synthesized at MMA concentration 0.5 phr. PMMA mass uptake has significantly improved the compression strength and resistance against thermooxidation with simultaneous decrease in their Rockwell hardness (R scale), charpy impact, and tensile strength of E/PMMA blends, respectively. With PMMA mass uptake, thermooxidative stability, thermal properties, and char yield of all such E/PMMA blends were increased.

The supercritical processing, thermal, spectral, and morphological characterization has been executed by the author Ms. Navdeep Bhullar for her special problem for post graduate research.

References

1. Nalawade, S. P.; Picchioni, F.; Janssen, L. P.; Prog, B. M. Prog Polym Sci 2006, 31, 19.
2. Cooper, A. I. J Mater Chem 2000, 10, 207.
3. Lee, S.; Lanterman, H.; Bryan, P.; Paul, Jr., F.; Kathy, L. U.S. Pat. 6,340,722 (2002).
4. Elkovitch, M. D.; Lee, L. J.; Tomasko, D. L. Polym Eng Sci 2000, 40, 1850.
5. Tang, M.; Wen, T. Y.; Du, T. B.; Chen, Y. P. Eur Polym J 2003, 39, 143.
6. Yuning, C.; Qun, X.; Minying, L.; Yudong, W.; Qingxiang, Z. J Appl Polym Sci 2003, 90, 2040.
7. Peng, Q.; Xu, Q.; Xu, H.; Pang, M.; Li, J.; Sun, D. J Appl Polym Sci 2005, 98, 864.
8. Chang, Y.; Xu, Q.; Liu, M.; Wang, Y.; Zhao, Q. J Appl Polym Sci 2003, 90, 2040.
9. Berg, V. E. A.; Christian, M. E. B.; Fortuyn, J. E.; van der Ree M. C. A.; Venderbosch, R. W.; Viersen, F. J.; Wit, G.; Wang, D. H.; Jana, S. C.; Andrew, J. S.; Caraher, J. M. U.S. Pat. 6,197,898 (2001).
10. Zhou, H.; Fang, J.; Yang, J.; Xie, X. J Supercritical Fluids 2003, 26, 137.
11. Lu, A.; Zhang, Z.; Nawaby, V.; Day, M. J Appl Polym Sci 2004, 93, 1236.
12. Maric, M.; Macosko, C. W. Polym Eng Sci 2001, 41.
13. Gombos, Z.; Mihályvas, V. L. N.; Gaál, J. Periodical Polytech Ser Mech Eng 2005, 49, 131.
14. Singh, V. P.; Zaidi, M. G. H. Proceedings of the International Conference on Recent Advances on Composites, Banaras Hindu University, BHU, India, 2004; pp 33–37.
15. Yupapin, P. V. P.; Kusamran, S. Smart Mater Struct 1993, 2, 157.
16. Joshi, S. K.; Kapil, J. C.; Rai, A. K.; Zaidi, M. G. H. Phys Status Solidi 2003, 199, 321.
17. Silverstein, R. M.; Webster, F. X.; Spectrophotometric Identification of Organic Compounds, 6th ed.; 1998; Chapter 3, pp 87–91.
18. Fang, J.; Kong, X. M.; Guo, B. H.; Hu, P.; Xie, X. M. Chem J Chin Univ 2001, 22, 151.
19. Tager, A. Physical Chemistry of Polymers; Mir Publishers: Moscow, 1978; p 162.
20. Kynin, A. T.; Grebennikov, S. F.; Perepelkin, K. E. Fibre Chem 1995, 27, 215.